Structural optimization of MTJs with a composite free layer

Alexander Makarov, Viktor Sverdlov, and Siegfried Selberherr
Institute for Microelectronics, TU Wien, Gußhausstraße 27-29, 1040 Wien, Austria

ABSTRACT

We investigate the switching statistics dependence on cell geometry by means of systematic micromagnetic simulations. We find that MTJs with a free layer composed of two ellipses with the axes *a/2* and *b* inscribed into a rectangle $a \times b$ are characterized by the same switching speed and thermal stability as MTJs with a composite free layer (C-MTJs). As has been shown, the C-MTJs demonstrate a substantial decrease of the switching time and the switching current as compared to conventional MTJs with a monolithic free layer. Thus, while preserving all the advantages of the C-MTJs, the newly proposed structure does not require a narrow gap between the two parts of the composite layer and therefore can be easily fabricated.

Keywords: MTJ, micromagnetic modeling, STT-MRAM, composite free layer

1. INTRODUCTION

Magnetoresistive random access memory with spin transfer torque (STT-MRAM) is a promising candidate for future universal memory [1-3]. The basic element of an MRAM is a pillar, a sandwich of two magnetic layers (Fig.1) separated by a non-magnetic metal (giant magnetoresistance (GMR) based devices) or a thin insulating oxide (magnetic tunnel junction (MTJ)). While the magnetization of the pinned layer is fixed due to the fabrication process, the magnetization direction of the free layer can be switched between the two states parallel and anti-parallel to the fixed magnetization direction.

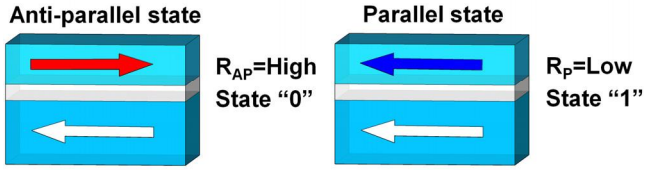

Figure 1. Schematic illustration of a three-layer MTJ in a high resistance (left) and low resistance (right) state.

1.1 Perpendicular vs. in-plane magnetization

Depending on the orientation of the magnetizations the magnetic pillars can be divided into two categories: "perpendicular" with out-of-plane magnetization direction and "in-plane" with magnetization lying in the plane of the magnetic layer.

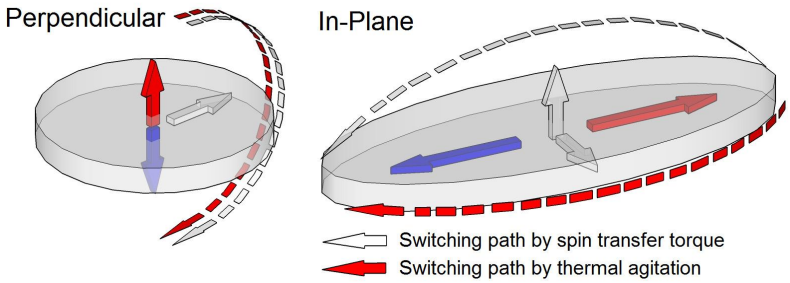

Figure 2. Schematic illustration of the free layer with a "perpendicular" magnetization (left) and "in-plane" magnetization direction (right).

In conventional field-driven MRAM the free layer magnetization switching is performed by applying a magnetic field. In contrast to field-driven MRAM, STT-MRAM does not require an external magnetic field. Switching between the two

Spintronics VI, edited by Henri-Jean Drouhin, Jean-Eric Wegrowe, Manijeh Razeghi, Proc. of SPIE Vol. 8813, 88132Q · © 2013 SPIE
CCC code: 0277-786X/13/$18 · doi: 10.1117/12.2025568

states occurs due to spin transfer torque produced by the spin-polarized current flowing through the pillar. The theoretical prediction of the spin transfer torque effect was made independently by Slonczewski [4] and Berger [5]. When electrons pass through the thick fixed magnetic layer, the spins of the electrons become aligned with the magnetization of this layer. When these spin-polarized electrons enter the free layer, their spin orientations are getting aligned with the magnetization of the free layer within a transition layer of a few angstroms. Because of their spin orientation changed in the free layer, they exert a torque on the magnetization of the layer, which can cause magnetization switching, if the torque is large enough to overcome damping. Smaller torque values result in magnetization precession around the effective magnetic field.

The spin-polarized current is only a fraction of the total charge current flowing through the device. Therefore, high current densities from ~10^7 to ~10^8 A/cm^2 are required to switch the magnetization direction of the free layer, and the reduction of this current density required for switching is the most important engineering challenge for these devices.

Switching of the magnetization can occur not only under the influence of the spin-polarized current, but also spontaneously due to thermal fluctuations (Fig.2). This is an unwanted event which leads to the loss of stored information. Thus another important parameter of MRAM (STT-MRAM) is the thermal stability factor which is defined as the ratio of the thermal stability barrier to the operating temperature.

The thermal stability factor for perpendicular MTJs (p-MTJs) is given by the interface-induced perpendicular anisotropy field H_K^{perp} as [6, 7]:

$$\Delta_{perp} = \frac{M_S \cdot \left(H_K^{perp} - 4\pi M_S\right) \cdot V}{2k_B T} \tag{1}$$

M_S is the saturation magnetization, V is the volume of the free layer, k_B is the Boltzmann constant. To increase the thermal stability factor it is sufficient to increase the cross-section of p-MTJs, however, due to domain formation, this is limited to approximately 70nm diameter, and therefore increasing the thermal stability factor of the single free layer p-MTJs above ~40-50 is a big challenge [8, 9].

In p-MTJs the switching paths by spin transfer torque and thermal agitations (Fig.2, left) are the same. Thus, the critical switching currents for p-MTJs are proportional to the thermal stability factor.

The thermal stability factor for in-plane MTJs is determined by the shape anisotropy field $H_K^{in-plane}$ [6, 7]:

$$\Delta_{in-plane} = \frac{M_S \cdot H_K^{in-plane} \cdot V}{2k_B T} \tag{2}$$

Therefore, to increase the thermal stability factor it is sufficient to increase the thickness of the free layer and/or the aspect ratio. However, switching under the influence of the spin current is following a different path than under the thermal agitations (Fig.2, right). Along this path the magnetization must get out of plane. Therefore, the switching energy barrier is mainly determined by the demagnetization energy contribution. This leads to an additional large term $2\pi M_S^2 V$ in the switching current

$$j_c^{in-plane} \propto M_S \cdot V \cdot \left(H_K^{in-plane} + 2\pi M_S\right) = 2k_B T \Delta_{in-plane} + 2\pi M_S^2 V\,, \tag{3}$$

which results in a higher critical current density compared to that in p-MTJs [6, 7].

Therefore, the in-plane MTJs exhibit a high thermal stability, but still require a reduction of the critical current density. Perpendicular MTJs with an interface-induced anisotropy show potential, but still require a reduction of damping and an increase of thermal stability. Thus, the research of finding new materials and architectures for MTJ structures is urgently needed.

1.2 MTJ with composite free layer

A penta-layer MTJ with a composite free layer (C-MTJ) was recently proposed [10]. The composite magnetic layer consists of two half-ellipses separated by a non-magnetic spacer (Fig.3). The magnetization of the magnetic layers lies in-plane. This allows to broaden substantially, as compared to p-MTJs, the scope of the magnetic materials suited for constructing MTJs.

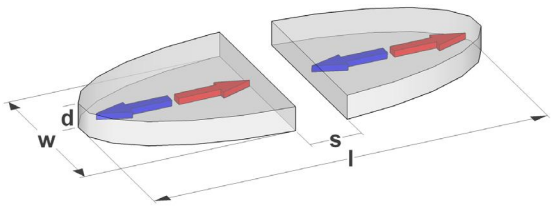

Figure 3. Schematic illustration of the composite free layer.

The C-MTJs demonstrate a substantial decrease of the switching time (Fig.4) and switching current as compared to the conventional MTJs with a monolithic free layer [11]. Fig.4 shows the decrease of the switching time in C-MTJs compared to that of conventional MTJs with a monolithic free layer of similar dimensions, for all cross section areas. The aspect ratio is chosen so that for a composite free layer ((*length-separation*)/2)/*width*=1.25. Each point is a result of statistical averaging with respect to 50 different realizations of the switching process. Our results clearly show a linear dependence of the switching time in the composite structures on the ratio *length*/*separation*.

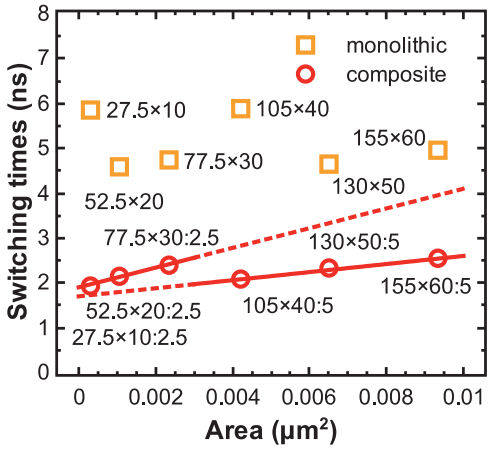

Figure 4. Average value of the switching times for conventional monolithic MTJs (*length*×*width*) and composite C-MTJs (*length*×*width*:*separation*) as function of the cross section area. Each point is a result of statistical averaging with respect to 50 different realizations of the switching process.

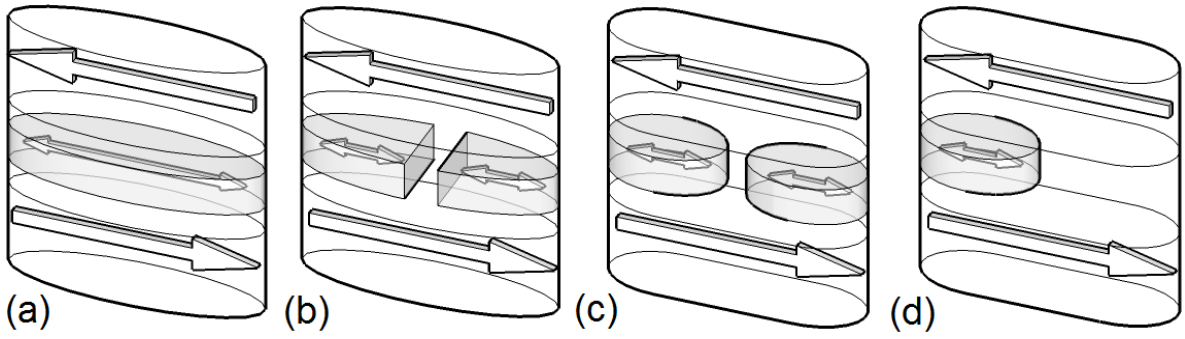

Figure 5. Schematic illustration of penta-layer MTJs with monolithic free layer (a) and M2-MTJ (d), and composite free layer C-MTJ (b) and C2-MTJ (c).

In this work we present a structural optimization of C-MTJs (Fig.5b) by means of extensive micromagnetic simulations and propose a new structure of the composite free layer, C2-MTJ (Fig.5c). We compared the most important parameters of STT-MRAM devices, as switching time, thermal stability, and switching energy barrier with C2-MTJ and C-MTJ, conventional MTJ (Fig.5a), and M2-MTJ (Fig.5d) structure.

2. MODEL DESCRIPTION

Our simulations of penta-layer MTJ switching are based on the magnetization dynamics described by the Landau-Lifschitz-Gilbert (LLG) equation with additional spin torque terms [12]:

$$\begin{aligned}\frac{dm}{dt} &= -\frac{\gamma}{1+\alpha^2}\cdot\Big(\big(m\times h_{eff}\big)+\alpha\cdot\big[m\times\big(m\times h_{eff}\big)\big]\\ &+\frac{g\mu_B j}{e\gamma M_s d}\cdot\big(g(\theta_1)\cdot\big(\alpha\cdot(m\times p_1)-[m\times(m\times p_1)]\big)\\ &-g(\theta_2)\cdot\big(\alpha\cdot(m\times p_2)-[m\times(m\times p_2)]\big)\Big)\Big)\end{aligned} \tag{4}$$

Here, γ=2.3245·10^{5}m/(A·s) is the gyromagnetic ratio, α is the Gilbert damping parameter, μ_B is the Bohr magneton, j is the current density, e is the electron charge, d is the thickness of the free layer, $m=M/M_s$ is the position dependent normalized vector of the magnetization in the free layer, $p_1=M_{p1}/M_{sp1}$ and $p_2=M_{p2}/M_{sp2}$ are the normalized magnetizations in the first and second pinned layers, respectively. M_s, M_{sp1}, and M_{sp2} are the saturation magnetizations of the free layer, the first pinned layer, and the second pinned layer, correspondingly. We use Slonczewski's expressions for the MTJ with a dielectric layer [13]:

$$g(\theta)=0.5\cdot\eta\cdot\left[1+\eta^2\cdot\cos(\theta)\right]^{-1} \tag{5}$$

The local effective field is calculated as [3]:

$$h_{eff}=h_{ext}+h_{ani}+h_{exch}+h_{demag}+h_{th}+h_{amp}+h_{ms} \tag{6}$$

Here, h_{ext} is the external field, h_{ani} is the magnetic anisotropy field, h_{exch} is the exchange field, h_{demag} is the demagnetizing field, h_{th} is the thermal field, h_{amp} is the Ampere field, and h_{ms} is the magnetostatic coupling field between the pinned and the free layers.

3. RESULT AND DISCUSSION

The simulations are performed for a nanopillar CoFeB/ MgO(1nm)/ CoFeB/ MgO(1nm)/ CoFeB MTJ, for a broad range of elliptical cross sections and different thicknesses of the pinned layers and the free layer. The other model parameters are: T=300K, $M_s=M_{sp}$=8.9·10^{5}A/m, A=1·10^{-11}J/m, K=2·10^3 J/m^3, α=0.005, and η=0.63 [14].

3.1 Switching time

First we study the switching times of C2-MTJs and compare it with those of C-MTJs. Fig.6 shows the dependence of the switching time on thicknesses of the free layer for three values of the short axis: 10nm, 15nm, and 20nm. The long axis is fixed at 52.5nm. Our simulations demonstrate that C2-MTJs and C-MTJs have practically equal switching times for all considered cross-sections of the free layer.

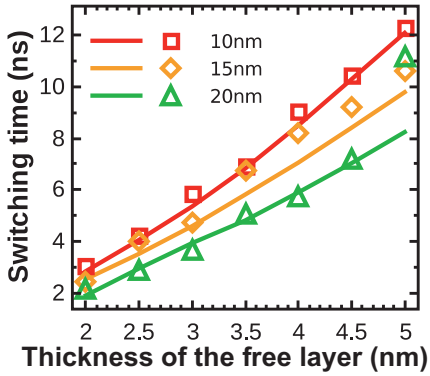

Figure 6. Switching time of C-MTJs (symbols) and C2-MTJs (lines) as function of the thickness of the free layer. The long axis is fixed at 52.5nm and the thickness of the fixed layer is 5nm. Dependences are shown for short axes of 10nm, 15nm, and 20nm length. Each point is a result of statistical averaging with respect to 30 different realizations of the switching process.

The fact that the switching times in C-MTJs and C2-MTJs are equal must result in switching acceleration for C2-MTJs as compared to the conventional MTJ with a monolithic free layer. This is indeed confirmed by the results of our simulations shown in Fig.7 (left). Fig.7 (right) demonstrates that C2-MTJs display almost the same switching times as the structure with a single small ellipse (M2-MTJ, Fig.5(d)).

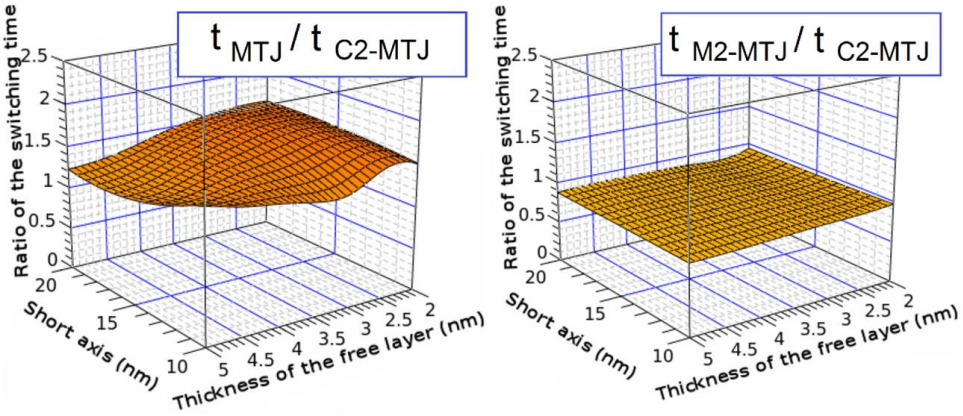

Figure 7. Ratio of the switching times in the monolithic structure and composite structure as function of thickness of the free layer and short axis length. The long axis is fixed at 52.5nm. Dependences are shown for ratio: conventional MTJ vs. C2-MTJ (left), M2-MTJ vs. C2-MTJ (right).

3.2 Thermal stability factor

We compare now the thermal stability factor for two types of composite layer structures: C-MTJ and C2-MTJ. Fig. 8 (left) confirms that the replacement of the free layer consisting of the two half-ellipses separated with a narrow gap (C-MTJ) by only two small ellipses (C2-MTJ), does not result in a loss of thermal stability. With $52.5\times10\text{nm}^2$ cross section and 5nm thickness of the free layer a thermal stability factor ~$60k_BT$ is obtained, which exceeds that of the single free layer p-MTJ demonstrated so far [8].

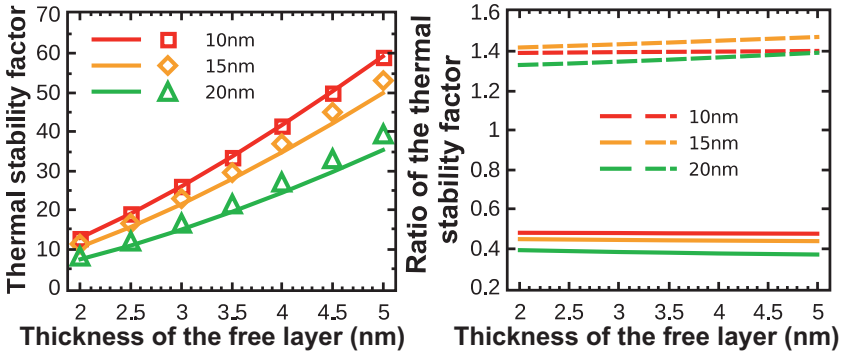

Figure 8. (left) Thermal stability factor for C-MTJ (symbols) and C2-MTJ (lines) as function of the thickness of the free layer. Each point is a result of statistical averaging with respect to 30 different realizations of the switching process. (right) Ratio of the thermal stability factors for monolithic structure and composite structure as function of thickness of the free layer and short axis length. Dependences are shown for ratio: M2-MTJ to C2-MTJ (solid lines), conventional MTJ to C2-MTJ (dotted lines). The long axis is fixed at 52.5nm and the thickness of the fixed layer is 5nm. Dependences are shown for short axes of 10nm, 15nm, and 20nm length.

Next we compare the thermal stability factor for C2-MTJ with that of the two structures with monolithic free layer: conventional MTJ and M2-MTJ. Due to the removal of the central region from the monolithic structure the shape anisotropy in the C2-MTJ is decreased together with the thermal stability factor (Fig.8, right). The constant ratio of the

thermal stability factor as a function of the aspect ratio and thicknesses of the free layer indicates that the thermal stability factors for both structures scales similarly. This means that in order to increase the thermal stability factor in C2-MTJs it is sufficient to increase the thickness of the free layer and/or the aspect ratio.

In comparison to the second structure with monolithic free layer, M2-MTJ, the C2-MTJ structure shows a gain in thermal stability by a factor of ~2 times (Fig.8, right), while maintaining the same switching time (Fig.7, right), confirming the superiority of the C2-MTJ structure over the M2-MTJ one.

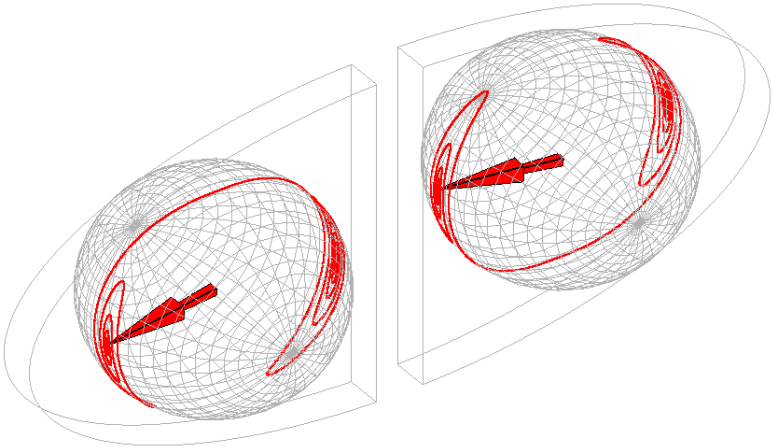

Figure 9. Illustration of the switching paths of magnetization in each piece of the composite C-MTJ structure under the influence of spin-polarized current.

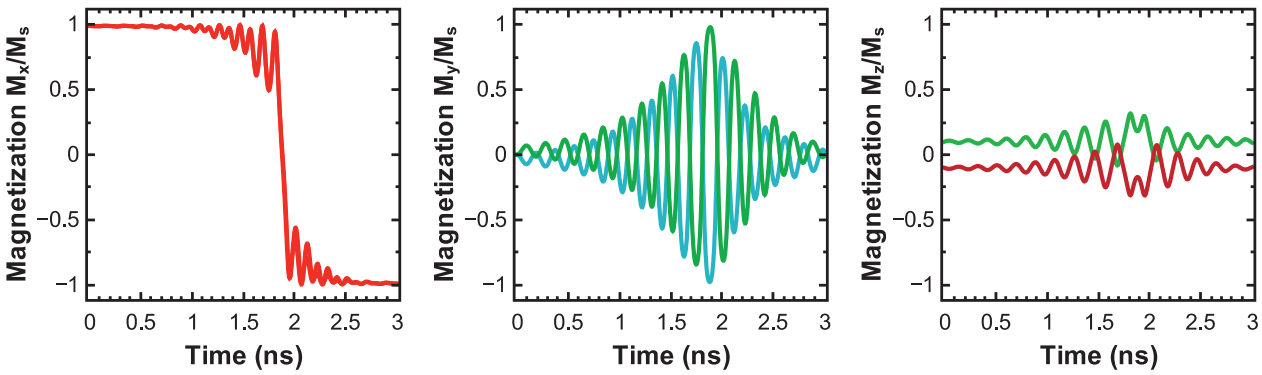

Figure 10. Magnetization components along the long axis (left), along the short axis (middle), and along the axis perpendicular to the free layer (right) as a function of time for a MTJ element of 52.5×20nm^2 size with a composite free layer (C2-MTJ). The magnetization of the left and right half is shown separately.

3.3 Switching energy barrier

To reveal the reason for fast switching we looked at the magnetization dynamics of the left and right part of the C-MTJ structure separately [15]. Fig.9 shows that the switching processes of the left and right part of the C-MTJ free layer occur in opposite senses to each other. Most importantly, the magnetizations of each piece stay in-plane. This switching behavior should lead to a decrease of the switching energy barrier. It turns out that the switching paths by current and due to thermal fluctuations are similar. Thus, as in p-MTJs, the switching barrier in a C-MTJ becomes practically equal to the thermal stability barrier defined by the shape anisotropy of the C-MTJ free layer. Reduction of the switching barrier leads to the reduction of the switching time in a C-MTJ as compared to a conventional MTJ at the same switching current density.

To determine the reason of the fast switching in C2-MTJs we also looked at the switching process in detail [11, 16]. Fig.10 shows that, as in a C-MTJ, the switching processes of the left and right part of the C2-MTJ free layer occur in opposite senses to each other. Importantly, the switching occurs in the *x*-*y* plane. This is clearly seen at the time instance 1.9ns, when the left and right ellipses pass simultaneously through the state (0; -1; 0) and (0; 1; 0) respectively (Fig.10).

In the following we compare the height of the thermal energy barrier with that of the switching energy barrier (Fig.11). As expected from the analysis of the magnetization dynamics, the switching barrier becomes practically equal to the thermal stability barrier in both C-MTJ and C2-MTJ structures. We note that the C2-MTJ structure posesses a lower switching barrier as compared to the C- MTJ structure with the same aspect ratio of the free layer.

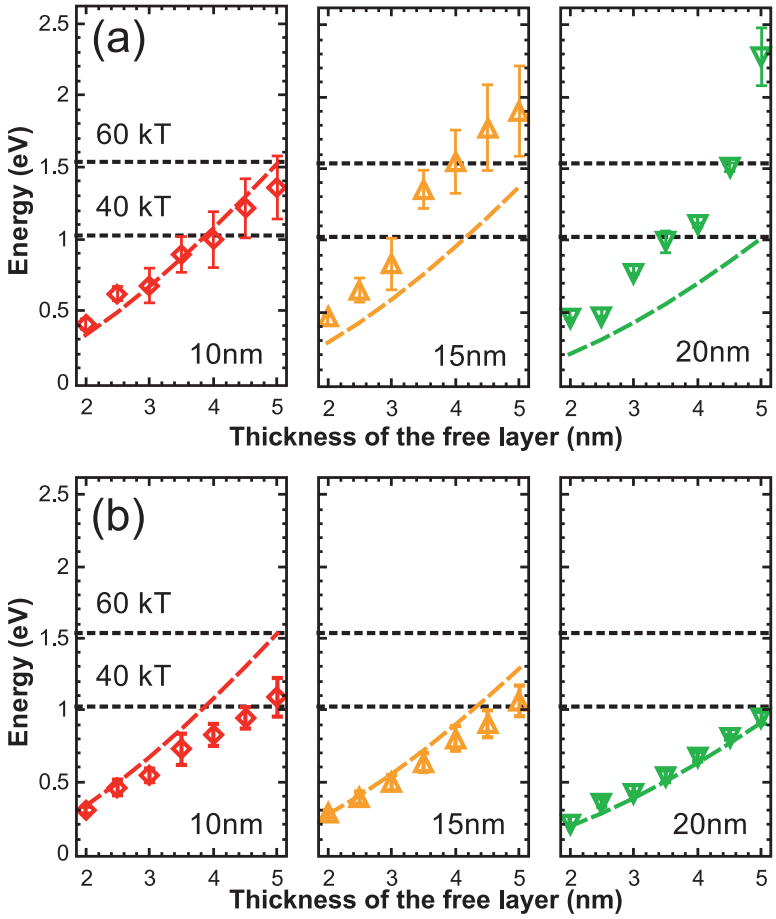

Figure 11. Thermal energy (lines) vs. switching energy (symbols) barriers for C-MTJs (a) and C2-MTJs (b). The long axis is fixed at 52.5nm and the thickness of the fixed layer is 5nm. Dependences are shown for short axes of 10nm, 15nm, and 20nm length. Each point is a result of statistical averaging with respect to 30 different realizations of the switching process.

3.4 Switching time distribution

The ratio of the standard deviations of the switching time distributions in the conventional MTJ and the composite C-MTJ structure is shown in Fig.12 (left). The width of the switching time distribution for C-MTJs can be almost ~2000 times narrower than that for conventional MTJs [16].

In order to find a physical explanation for the switching time distribution narrowing, we again analyze the switching process in detail. A schematic illustration of the self-stabilization and self-acceleration principle of switching in a

composite free layer is shown in Fig.12 (right). Each half of the free layer generates a stray magnetic field which influences the other half and helps stabilizing the switching process. This stray magnetic field increases with increasing short axis, which leads to the switching times distribution narrowing. At the moment, when the magnetizations in two different halves of the composite layer are in opposite directions to each other (Fig.12b), this stray magnetic field acts as a stabilizing factor of switching (Fig.12a). After the opposite magnetization state is passed, the stray magnetic fields accelerate the switching as illustrated in Fig.12c.

Now we compare the standard deviations of the switching time distributions in C-MTJs and C2-MTJs. The dependence of the value of the standard deviation on composite layer thickness and aspect ratio is shown in Fig.13. With 52.5×25nm^2 cross section a standard deviation of the switching time ~10^{-3}ns is obtained for both structure, while with 52.5×10nm^2 cross section the standard deviation of the switching time is 0.3-1.6ns for the C-MTJ and 0.09-0.9ns for the C2-MTJ. Thus the C2-MTJ structure shows a ~2-3 times narrower distribution of the switching time as compared to the C-MTJ structure at large aspect ratio of the free layer.

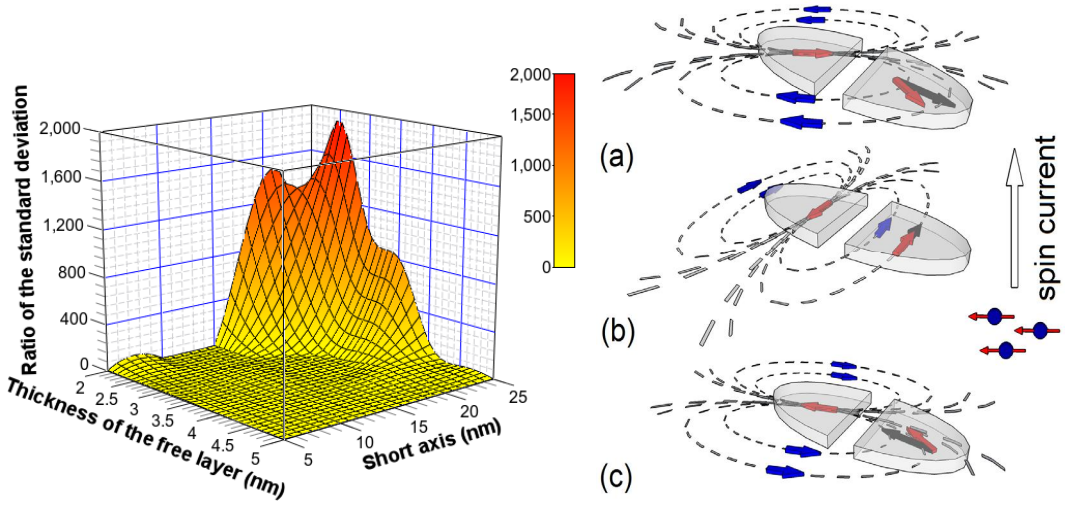

Figure 12. (left) Ratio of the standard deviation of the switching time in the conventional MTJ structure and the C-MTJ structure as function of thickness of the free layer and short axis length. The long axis is fixed at 52.5nm and the thickness of the fixed layer is 10nm. (right) Schematic illustration of the state with self-stabilization direction of the stray magnetic field (a), opposite magnetization state (b), and self-acceleration switching state (c) in the C-MTJ structure.

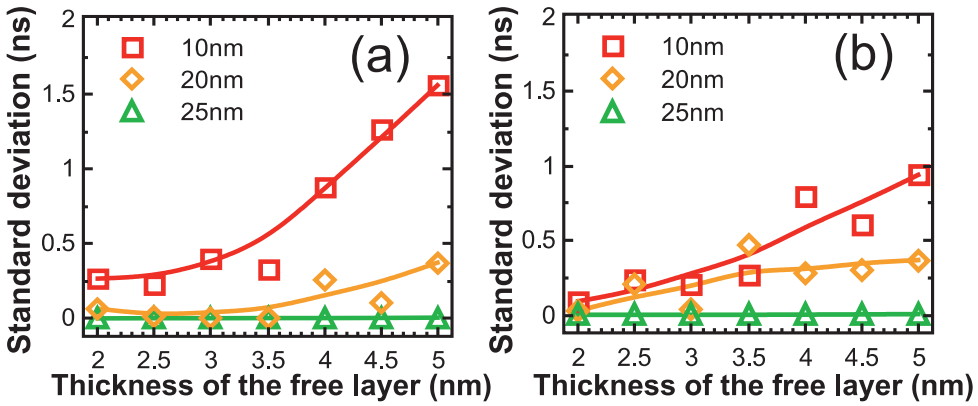

Figure 13. The standard deviation of the switching time distribution in the C-MTJ structure (a) and the C2-MTJ structure (b) as function of thickness of the free layer. The long axis is fixed at 52.5nm and the thickness of the fixed layer is 15nm. Dependences are shown for the short axis of 10nm, 20nm, and 25nm. Each point is a result of statistical averaging with respect to 30 different realizations of the switching process.

4. CONCLUSION

We proposed and analyzed a new C2-MTJ structure with a composite free layer consisting of two ellipses with the axes *a/2* and *b* inscribed into a rectangle $a \times b$. Our simulations show that, while preserving all the advantages of the C-MTJ structure, such as fast switching, high thermal stability factor, and very narrow distribution of switching times, the newly proposed structure can be easier fabricated, offering a greater potential for the STT-MRAM performance optimization.

REFERENCES

[1] Dorrance, R., Ren, F., Toriyama, Y., Hafez, A. A., Yang, C-K. K., and Marković, D., "Scalability and design-space analysis of a 1T-1MTJ memory cell for STT-RAMs," IEEE Trans. on Electron Dev. 59, 878-887 (2012).

[2] Gajek, M., Nowak, J. J., Sun, J. Z., Trouilloud, P. L., O'Sullivan, E. J., Abraham, D. W., Gaidis, M. C., Hu, G., Brown, S., Zhu, Y., Robertazzi, R. P., Gallagher, W. J., and Worledge, D. C., "Spin torque switching of 20nm magnetic tunnel junctions with perpendicular anisotropy," Appl. Phys. Lett. 100, 132408 (2012).

[3] Makarov, A., Sverdlov, V., and Selberherr, S., "Emerging memory technologies: trends, challenges, and modeling methods," Microelectronics Reliability 52, 628 – 634 (2012).

[4] Slonczewski, J., "Current-driven excitation of magnetic multilayers," J. Magn. Magn. Mater. 159, L1 (1996).

[5] Berger, L., "Emission of spin waves by a magnetic multilayer traversed by a current," Phys Rev. B 54, 9353 (1996).

[6] Apalkov, D., Watts, S., Driskill-Smith, A., Chen, E., Zhitao, D., Nikitin, V., "Comparison of scaling of In-Plane and Perpendicular spin transfer switching technologies by micromagnetic simulation," IEEE Trans. on Mag. 46 (6), 2240 (2010).

[7] Sbiaa, R., Lua, S. Y. H., Law, R., Meng, H., Lye, R., and Tan, H. K., "Reduction of switching current by spin transfer torque effect in perpendicular anisotropy magnetoresistive devices," J. Appl. Phys. 109, 07C707 (2011).

[8] Sato, H., Yamanouchi, M., Miura, K., Ikeda, S., Gan, H. D., Mizunuma, K., Koizumi, R., Matsukura, F., and Ohno, H., "Junction size effect on switching current and thermal stability in CoFeB/MgO perpendicular magnetic tunnel junctions," Appl. Phys. Lett. 99, 042501 (2011).

[9] Sato, H., Yamanouchi, M., Ikeda, S., Fukami, S., Matsukura, F., and Ohno, H., "Perpendicular-anisotropy CoFeB-MgO magnetic tunnel junctions with a MgO/CoFeB/Ta/CoFeB/MgO recording structure," Appl. Phys. Lett. 101, 022414 (2012).

[10] Makarov, A., Sverdlov, V., and Selberherr, S., "Reduction of switching time in pentalayer magnetic tunnel junctions with a composite-free layer," Phys. Stat. Solidi RRL 5, 420-422 (2011).

[11] Makarov, A., Sverdlov, V., and Selberherr, S., "MTJs with a composite free layer for high-speed spin transfer torque RAM: micromagnetic simulations," Proc. IWCE, 1-4 (2012).

[12] Makarov, A., Osintsev, D., Sverdlov, V., and Selberherr, S., "Fast switching in magnetic tunnel junctions with two pinned layers: micromagnetic modeling," IEEE Trans. on Mag. 48 (4), 1289-1292 (2012).

[13] Slonczewski, J., "Currents, torques, and polarization factors in magnetic tunnel junctions," Phys. Rev. B 71, 024411 (2005).

[14] Iwayama, M., Kai, T., Nakayama, M., Aikawa, H., Asao, Y., Kajiyama, T., Ikegawa, S., Yoda, H., and Nitayama, A., "Reduction of switching current distribution in spin transfer magnetic random access memories," J. Appl. Phys., 103, 07A720 (2008).

[15] Makarov, A., Sverdlov, V., and Selberherr, S., "Magnetic tunnel junctions with a composite free layer: a new concept for future universal memory," [Future Trends in Microelectronics - Frontiers and Innovations], S. Luryi, J. Xu, A. Zaslavsky (ed.), John Wiley & Sons, 93-101 (2013).

[16] Makarov, A., Sverdlov, V., and Selberherr, S., "Study of self-accelerating switching in MTJs with composite free layer by micromagnetic simulations," Proc. SISPAD, 229-232 (2012).

Acknowledgment

This work is supported by the European Research Council through the grant #247056 MOSILSPIN.